A STRUCTURAL MODEL OF THE LAYER TITANOSILICATE BORNEMANITE BASED ON SEIDOZERITE AND LOMONOSOVITE MODULES

GIOVANNI FERRARIS[§], ELENA BELLUSO AND ANGELA GULA

Dipartimento di Scienze Mineralogiche e Petrologiche, Università di Torino, Via Valperga Caluso, 35, I-10125, Torino, Italy

SVETLANA V. SOBOLEVA, OLGA A. AGEEVA AND BORIS E. BORUTSKII

Institute of Ore Deposits, Petrography, Mineralogy and Geochemistry, Moscow 109017, Russia

ABSTRACT

Bornemanite is a rare alkali titanosilicate occurring in the natrolite zone of the Yubileynaya hyperagpaitic pegmatite, on Karnasurt Mountain, in the Lovozero massif, Kola Peninsula, Russia. The mineral is light yellow, lamellar (001) and elongate [010]. No single crystals suitable for X-ray crystallography are available. New electron-microprobe chemical analyses, selected-area electron diffraction (SAED) and X-ray powder diffraction show that bornemanite, $BaNa_3\{(Na,Ti)_4[(Ti,Nb)_2O_2Si_4O_{14}](F,OH)_2\}PO_4$, is monoclinic $I11b$, a 5.498(4), b 7.120(6), c 47.95(4) Å, γ 88.4(1)°; $Z = 4$. By comparison with structural and chemical data for titanosilicates based on a bafertisite-like layer (heterophyllosilicates), a model of the structure of bornemanite has been obtained. This model has been refined by the distance least-squares technique (DLS program) and tested against calculated powder-diffraction and SAED patterns. The structure of bornemanite can be described as a [001] stacking of heterophyllosilicate layers, where lomonosovite and seidozerite contents alternate in the interlayer spaces. Thus this structure is the first documented case of a heterophyllosilicate based on modules of two other structures belonging to the same modular series, *i.e.*, the mero-plesiotype bafertisite series. The lomonosovite–seidozerite polysomatic series is defined. In contrast to the original description, bornemanite is considered monoclinic and not orthorhombic, and lacks one cation per formula unit (mainly Na). Possible leaching of alkalis and the solid-state oriented transformation lomonosovite → bornemanite are discussed.

Keywords: bornemanite, new data, crystal structure, heterophyllosilicate, Lovozero massif, Kola Peninsula, Russia.

SOMMAIRE

La bornemanite, titanosilicate rare à alcalins, provient de la zone à natrolite de la pegmatite hyperagpaïtique de Yubileynaya, sur le mont Karnasurt, faisant partie du complexe de Lovozero, péninsule de Kola, en Russie. Le minéral est jaune pâle, se présentant en lamelles (001) allongées selon [010]. Aucun cristal unique n'a été trouvé pour des études cristallographiques par rayons X. De nouvelles données sur la composition, obtenues avec une microsonde électronique, et sur la structure (diffraction des électrons sur aire sélectionnée, diffraction X sur poudre) montrent que la bornemanite, $BaNa_3\{(Na,Ti)_4[(Ti,Nb)_2O_2Si_4O_{14}](F,OH)_2\}PO_4$, serait monoclinique $I11b$, a 5.498(4), b 7.120(6), c 47.95(4) Å, γ 88.4(1)°; $Z = 4$. En comparaison avec les données structurales et chimiques sur les titanosilicates possédant une couche semblable à la bafertisite (hétérophyllosilicates), nous avons obtenu un modèle de la structure de la bornemanite. Nous avons pu affiner ce modèle en utilisant la technique des distances évaluées par moindres carrés (logiciel DLS) et le tester par comparaison avec les spectres calculés de diffraction sur poudre et de diffraction d'électrons. Nous décrivons la structure de la bornemanite en termes d'un empilement de couches de hétérophyllosilicate le long de [001] dans laquelle le contenu de lomonosovite et de seidozérite alternent dans les espaces interfoliaires. Cette structure serait donc le premier cas bien documenté d'un hétérophyllosilicate contenant des modules de deux autres structures faisant partie de la même série modulaire, c'est-à-dire la série de la bafertisite, à caractère méro-plésiotypique. On définit la série polysomatique de la lomonosovite–seidozérite. Contrairement à ce qui est déjà dans la littérature, la bornemanite serait monoclinique et non orthorhombique, et démontrerait une déficience d'un cation par unité formulaire, surtout Na. Nous abordons le sujet d'un lessivage possible des alcalins et d'une transformation orientée de la lomonosovite en bornemanite à l'état solide.

(Traduit par la Rédaction)

Mots-clés: bornemanite, nouvelles données, structure cristalline, hétérophyllosilicate, complexe de Lovozero, péninsule de Kola, Russie.

§   *E-mail address*: ferraris@dsmp.unito.it

INTRODUCTION

Bornemanite, $BaNa_3\{(Na,Ti)_4[(Ti,Nb)_2O_2Si_4O_{14}](F,OH)_2\}PO_4$, was discovered in the natrolite zone of the Yubileynaya pegmatite, Mount Karnasurt, Lovozero massif, Kola Peninsula, Russia (Men'shikov *et al.* 1975). Since then, two other bornemanite-bearing pegmatites belonging to the same massif, Shkatulka and Sirenevaya, have been found (Pekov 2000). According to Pekov (2000), lamellar bornemanite of Yubileynaya develops along cleavage planes of lomonosovite and occasionally completely replaces it. In the other two pegmatites mentioned, on the other hand, bornemanite occurs as spherulites associated with lomonosovite among other minerals; in the Sirenevaya pegmatite, bornemanite occasionally is seen also to replace lomonosovite. Because of the lack of suitable single crystals, the crystal structure of bornemanite remains unknown, even if similarities with layer titanosilicates were pointed out (Ferraris *et al.* 1997).

The availability of a sample (NH–10), originally collected by Yu.P. Men'shikov and conserved in the collection of the Institute of Ore Deposits, Petrography, Mineralogy and Geochemistry (IGEM, Moscow), prompted us to improve on the characterization of bornemanite. In this sample, millimetric (001) lamellar grains of light yellow bornemanite occur on the (001) faces of large crystals of lomonosovite. All attempts to find a single crystal of bornemanite suitable for X-ray diffraction failed. In order to obtain information with which to model the structure of bornemanite, we investigated sample NH–10 with a combination of X-ray and electron-diffraction methods, and characterized it by electron-microprobe analysis.

EXPERIMENTAL

The main experimental data were obtained with a Philips CM12 transmission electron microscope (TEM) (LaB_6 filament, operated at 120 kV; University of Torino), an electron microprobe ARL–SEMQ [operated in wavelength-dispersion (WDS) mode at 20 nA, 15 kV; University of Modena and Reggio Emilia] and a Philips X'Pert X-ray powder diffractometer ($CuK\alpha$ radiation; University of Milano).

TEM observation of the lamellar grains reveals that they consist of very thin laths (typically about 0.2 × 0.1 × 0.05 mm) that show a perfect {001} cleavage (Fig. 1c). At variance with Men'shikov *et al.* (1975), who reported [100] elongation on the basis of optical observations, our TEM study indicates a [010] elongation.

The results of the WDS electron-microprobe analyses reported in Table 1 represent 11 point analyses collected from two different grains. On the basis of 4 Si atoms per formula unit (*apfu*), and according to the model of structure discussed below, the following crystal-chemical formula is obtained: $(Na_{2.83}Ba_{0.71}K_{0.12}Sr_{0.06}Ca_{0.04}Mg_{0.01})_{\Sigma3.77}$ $\{(Na_{2.64}Ti_{1.00}Mn_{0.30}Fe_{0.03}$

$Al_{0.03})_{\Sigma4.00}$ $[(Ti_{1.27}Nb_{0.69}Zr_{0.01})_{\Sigma1.97}O_2Si_4O_{14}](O_{0.38}(OH)_{0.71}F_{0.62}Cl_{0.01})_{\Sigma1.72}\}(PO_4)_{0.82}$.

For this composition, a unit-formula weight of 904.26 and a calculated density D of 3.203 g/cm^3 are obtained ($Z = 4$). The density observed by Men'shikov *et al.* (1975) is in the range of 3.47–3.50 g/cm^3, significantly higher but presumably affected by the presence of aegirine impurities; the scarcity of sample NH–10 did not allow a new measurement. The significantly lower content of alkalis, by about 1 *apfu*, between the original data, 6.43(Na + K), and our average results, 5.59(Na + K), is likely due to the presence of lomonosovite impurities in the large amount of sample used for the original wet-chemical analysis (but see below). In the chemical formula, following Ferraris *et al.* (2001), the composition of the heterophyllosilicate layer (*HOH* layer, see below) is shown within braces, and that of the heteropolyhedral *H* sheet is given between square brackets; finally, the composition of the interlayer is represented by the part outside the braces.

The formula of our sample of bornemanite can be approximated as $BaNa_{2.5}Mn_{0.5}\{Na_3Ti[TiNbO_2Si_4O_{14}](O_{0.5}OH_{0.75}F_{0.75})\}PO_4$, for which the unit-formula weight MW is 978.24 and D(calc) is 3.46 g/cm^3 ($Z = 4$). The corresponding oxide composition, in wt%, is: SiO_2

TABLE 1. CHEMICAL COMPOSITION OF BORNEMANITE§

Oxides	Average	Range	Standard
SiO_2 wt%	26.42	25.63 – 26.97	Anorthite
Al_2O_3	0.15	0.13 – 0.18	Spessartine
CaO	0.26	0.22 – 0.30	Anorthite
SrO	0.72	0.60 – 0.92	Sr-substituted anorthite
BaO	12.02	11.44 – 12.76	Paracelsian
MnO	2.37	2.22 – 2.52	Spessartine
FeO	0.22	0.17 – 0.28	Ilmenite
Nb_2O_5	10.13	9.47 – 10.79	Metallic Nb
TiO_2	19.94	19.55 – 20.51	Ilmenite
ZrO_2	0.06	0.00 – 0.19	Metallic Zr
K_2O	0.61	0.55 – 0.69	Microcline
Na_2O	18.64	17.38 – 19.89	Albite
MgO	0.02	0.00 – 0.04	Forsterite
F	1.29	0.98 – 1.54	Fluorite
Cl	0.03	0.00 – 0.07	Sodalite
P_2O_5	6.44	5.82 – 6.90	Apatite
H_2O^*	0.7		
Total	100.02		
F = O	–0.54		
Cl = O	–0.01		
Total	99.47		

* Determined by thermogravimetry (Men'shikov *et al.* 1975).
§ Determined by electron-microprobe analysis.

FIG. 1. Experimental [100] (a) and [001] (d) SAED patterns of bornemanite compared with the corresponding calculated patterns (b, e and f). Both the *hk*0 plane alone (e) and the [001] projection of *hk*0 + *hk*1 + *hk*2 (f) are shown. The [001] SAED pattern (d) has been obtained from [010] elongate platelet shown in (c).
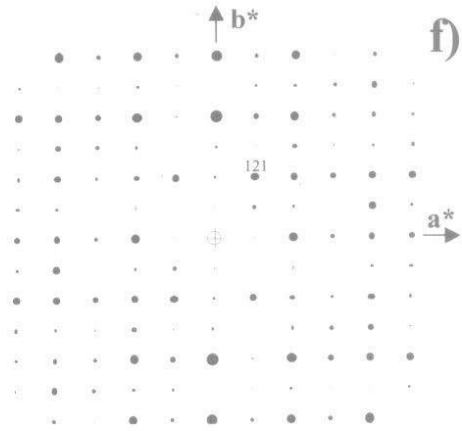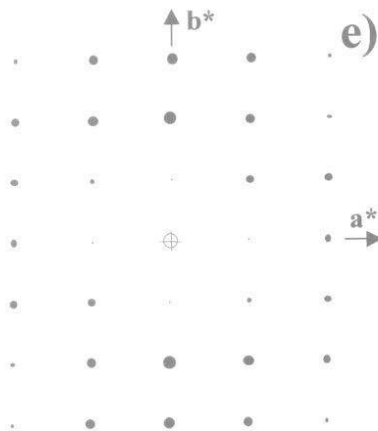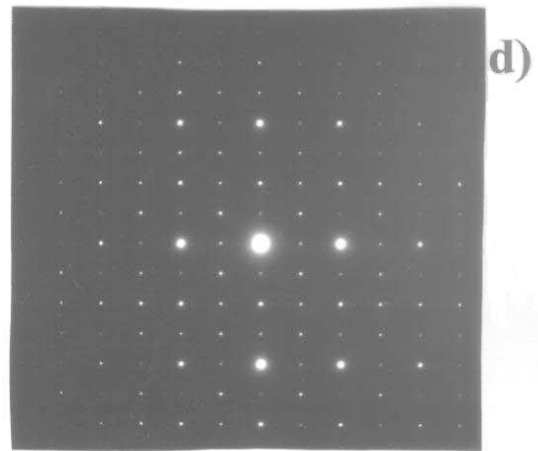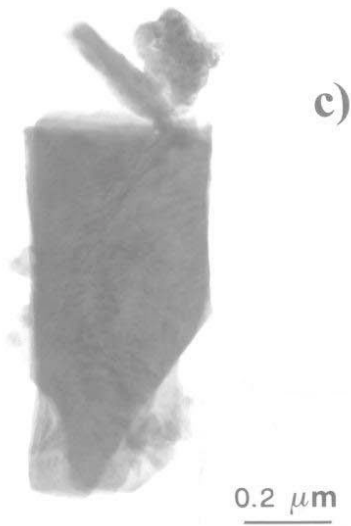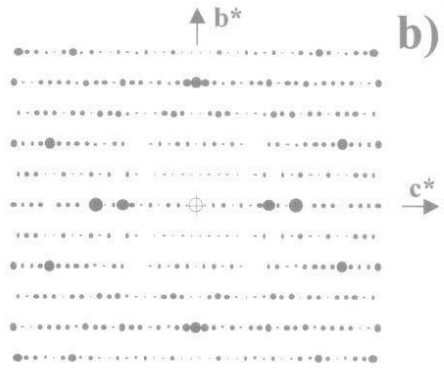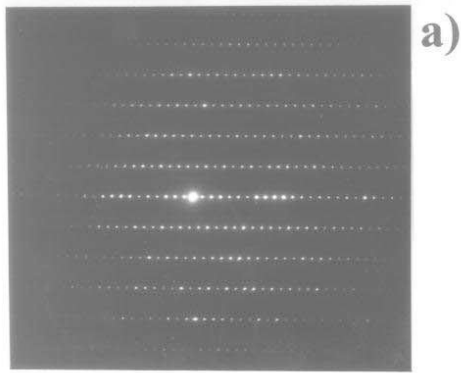
24.57, BaO 15.67, MnO 3.62, Nb_2O_5 13.58, TiO_2 16.33, Na_2O 17.42, F 1.45, P_2O_5 7.25 and H_2O 0.69. The H_2O content agrees well with the value obtained by thermogravimetry, 0.7% (Men'shikov *et al.* 1975). An ideal formula for bornemanite can be written as $BaNa_3\{(Na,Ti)_4[(Ti,Nb)_2O_2Si_4O_{14}](F,OH)_2\}PO_4$, to be compared with the ideal formula $BaNa_4Ti_2NbSi_4O_{17}$ $(F,OH)_2 \cdot Na_3PO_4$ proposed in the original description; thus bornemanite is poorer in cations (mainly Na) than originally reported. Apart from possible errors in the original wet-chemical analysis, the lower content of cations in our sample could be due to leaching of alkalis, as discussed for delindeite by Ferraris *et al.* (2001). Unfortunately, the availability of a structural model only, instead of a fully refined structure, does not allow a thorough discussion of this matter.

Selected-area electron diffraction (SAED) patterns have been obtained from two different orientations of the bornemanite (001) laths. (i) Electron beam along [100] (Fig. 1a): $b \approx 7.1$, $c \approx 48$ Å, $k + l = 2n$ and symmetry *cmm* are observed. (ii) Electron beam along [001] (Fig. 1d): $a \approx 5.5$, $b \approx 7.1$ Å, $\gamma \approx 89°$; reflections with even values of *h* and *k* are stronger than those with odd values. Owing to the small value of c^*, the latter reflections belong to the upper layers $hk1$ ($h + k = 2n + 1$) and $hk2$ ($h + k = 2n$); on the whole, the [001] SAED pattern shows an approximate symmetry *pmm*.

We conclude that bornemanite is monoclinic, and its electron-diffraction patterns show the following systematic absences: $h + k + l = 2n + 1$ (all reflections) and $k = 2n + 1$ (*hk0* reflections only). Thus, the space group is either $I112/b$ or $I11b$; the latter is consistent with the structure model discussed below. The unconventional choice of the space group, instead of the conventional $C1c1$, is adopted to maintain correspondence with related (001) layer titanosilicate structures (see below).

The following parameters for the *I*-centered cell have been obtained by refining the X-ray powder-diffraction data (Table 2), which were indexed by taking into account the intensities calculated from the structural model discussed below: *a* 5.498(4), *b* 7.120(6), *c* 47.95(4) Å, γ 88.4(1)°, *V* 1876 Å^3. These parameters are comparable to those published by Men'shikov *et al.* (1975) who, however, indicated *Ima2* as the possible spacegroup. The transformation matrix for the cell parameters from $I11b$ to the conventional $C1c1$ space group is /Ī10/001/100/. The cell parameters *a* 8.873, *b* 47.95, *c* 5.498 Å, β 126.67° are obtained for the *C*-centered cell; the very obtuse β angle of this cell is another reason for adopting the unconventional space-group $I11b$.

The Structural Model

The values of the cell parameters and the presence of the complex anion $[(Ti,Nb)_2O_2Si_4O_{14}]$ in the chemical formula support a strong analogy between bornemanite and the seidozerite-derivative titanosilicates (or bafertisite polysomatic series), as inferred by Ferraris *et*

al. (1997) and Ferraris (1997). The titanosilicates belonging to this series that have a known structure and that occur in the Lovozero massif (Khomyakov 1995,

TABLE 2. X-RAY POWDER-DIFFRACTION PATTERN OF BORNEMANITE: OBSERVED AND CALCULATED DATA

I_{obs}	I_{calc}	d_{obs}	d_{calc}	hkl
100	100	23.80	23.98	002*
2.5	2	12.00	12.03	004
92	44	8.02	7.99	006
1	9	7.05	7.04	011
2	11	6.51	6.50	013
1	4	6.02	5.99	008
2	5	5.80	5.72	015*
3	7	5.01	4.94	017*
8	3	4.82	4.80	00$\underline{10}$
2	1	4.76	4.77	105
3	1	4.34	4.34	112
6	3	4.29	4.29, 4.27	107, 019*
6	12	4.25	4.23	1$\bar{1}$2
4	5	4.08	4.14	114
13	16	4.02	4.04	1$\bar{1}$4
8	14	3.786	3.781	1$\bar{1}$6
7	3	3.695	3.717	01$\underline{11}$
7	2	3.568	3.559, 3.551	028, 118
7	2	3.509	3.520	022
63	41	3.447	3.490, 3.425, 3.415, 3.411	1$\bar{1}$8*, 00$\underline{14}$, 10$\underline{11}$, 024*
4	1	3.326	3.275	01$\underline{13}$*
4	3	3.285	3.251	026
5	6	3.230	3.246	1$\underline{110}$
6	2	3.188	3.198	1$\bar{1}\underline{10}$
7	8	3.080	3.063, 3.060	10$\underline{13}$, 028
94	70	3.016	3.020, 3.997, 2.973, 2.961	121, 00$\underline{16}$, 123*, 11$\underline{12}$*
10	17	2.951	2.944	1$\bar{2}$1
6	11	2.582	2.581	
10	9	2.909	2.886	125
12	6	2.833	2.858, 2.819	02$\underline{10}$*, 1$\bar{2}$5
13	12	2.772	2.768, 2.763	127, 10$\underline{15}$
24	17	2.705	2.730	202*
41	37	2.683	2.709, 2.705, 2.679, 2.677, 2.664	1$\bar{2}$7*, 11$\underline{14}$, 204, 1$\bar{1}$4, 00$\underline{18}$*
9	17	2.619	2.631	129
6	11	2.582	2.581	1$\bar{2}$9
4	5	2.527	2.536, 2.509	2$\bar{1}$1, 10$\underline{17}$*
3	4	2.475	2.479, 2.468	11$\underline{16}$, 02$\underline{14}$*
2	1	2.445	2.455	2$\bar{1}$5
17	21	2.410	2.443, 2.421	12$\underline{11}$*, 217
2	2	2.294	2.292	0$\bar{2}$16
1	7	2.245	2.242	037
6	4	2.153	2.179	00$\underline{22}$
3	2	2.088	2.069	228
8	5	2.027	2.063, 2.039, 2.029	12$\underline{17}$*, 1$\bar{2}\underline{17}$, 1$\bar{3}$8
11	8	2.013	2.011, 2.003, 2.001, 1.967	21$\underline{15}$, 22$\underline{10}$, 0$\bar{1}$23, 1$\bar{3}\underline{10}$*
1.5	1	1.897	1.898	1$\bar{3}$12
6	6	1.783	1.779	040
2	1	1.701	1.701	11$\underline{26}$
2	2	1.688	1.689, 1.681	30$\underline{11}$, 2$\bar{3}$9*
1.5	2	1.664	1.670	1$\bar{4}$3
2	2	1.643	1.641	30$\underline{13}$
2	1	1.630	1.633	23$\underline{13}$
7	6	1.610	1.611, 1.611, 1.610, 1.608	2$\bar{1}$23, 0$\bar{1}$29, 3$\bar{2}$1, 1$\bar{2}$25*
1.5	1	1.544	1.549	14$\underline{13}$
3	2	1.511	1.513, 1.511	240, 1$\bar{3}$$\underline{11}$
3	3	1.486	1.490, 1.487, 1.487	10$\underline{31}$, 14$\underline{15}$, 246
2	1	1.462	1.464	21$\underline{27}$
2	2	1.443	1.443	1$\bar{4}$$\underline{17}$
6	4	1.422	1.428, 1.427, 1.422, 1.419	04$\underline{20}$*, 338, 03$\underline{27}$, 11$\underline{32}$
1	1	1.393	1.399	2$\bar{2}$26
1	1	1.360	1.360	3$\bar{2}$19
2	2	1.342	1.343, 1.342	41$\underline{15}$, 4$\bar{1}$1
1	1	1.322	1.321	40$\underline{10}$
1	1	1.291	1.291	3$\bar{3}$16
1	1	1.255	1.256	2$\bar{4}$20

§ Cu*K*α radiation, graphite monochromator; 40 kV, 40 mA; range 2–80° 2θ, step-size 0.02° 2θ; scan-time 10 s/step. * Not used in the cell refinement. Values of *d* in Å.

TABLE 3. TITANOSILICATES OCCURRING IN THE LOVOZERO MASSIF
FOR WHICH THE STRUCTURE IS KNOWN AND BASED ON
A BAFERTISITE-LIKE HETEROPHYLLOSILICATE *HOH* LAYER

Mineral*	Formula	t (Å)	Reference**
Seidozerite	$Na_2\{(Na,Mn,Ti)_4[(Na,Ti,Zr)_2O_2Si_4O_{14}]F_2\}$	8.93	Simonov & Belov (1960)
Lamprophyllite	$(Sr,Ba)_2\{(Na(Na,Mn)_2Ti)[Ti_2O_2Si_4O_{14}](OH)_2\}$	9.80	Rastsvetaeva *et al.* (1990)
Barytolamprophyllite	$(Ba,Na)_2\{(Na,Ti,Fe,Ba)_4[Ti_2O_2Si_4O_{14}](OH,F)_2\}$	9.80	Peng *et al.* (1984)
Delindeite	$Ba_2\{(Na,\square)_3Ti[Ti_2(O,OH)_2Si_4O_{14}](H_2O,O,OH)_2\}$	10.73	Ferraris *et al.* (2001)
Murmanite	$Na_2\{(Ti,Na,\square)_4[Ti_2O_2(OH)_2Si_4O_{14}](O,OH)_2\}$	11.60	Rastsvetaeva & Andrianov (1986)
Bornemanite	$Na_3Ba\{(Na,Ti,Mn)_4[(Ti,Nb)_2O_2Si_4O_{14}](O,OH)_2\}(PO_4)$	11.99	This study
Vuonnemite	$Na_8\{(Na,Ti)_4[Nb_2O_2Si_4O_{14}](O,OH,F)_2\}(PO_4)_2$	14.40	Ercit *et al.* (1998)
Lomonosovite	$Na_8\{(Na,Ti)_4[Ti_2O_2Si_4O_{14}](O,F)_2\}(PO_4)_2$	14.48	Belov *et al.* (1978)
Quadruphite	$Na_{13}Ca\{(NaMgTi_2)[Ti_2O_2Si_4O_{14}]O_2\}(PO_4)_4F_2$	20.25	Khomyakov *et al.* (1992)
Sobolevite	$Na_{12}CaMg\{(NaMgTi_2)[Ti_2O_2Si_4O_{14}]O_2\}(PO_4)_4F_2$	20.28	Sokolova *et al.* (1988)
Polyphite	$Na_{14}(Ca,Mn,Mg)_5\{(Ti,Mn,Mg)_4[Ti_2O_2Si_4O_{14}]F_2\}(PO_4)_6F_4$	26.49	Khomyakov *et al.* (1992)

* The minerals are listed in order of increasing $t = d(001)/n$, with n corresponding to the number of *HOH* layers in the cell. ** Each reference reports the most recent structural paper.
The content of the heteropolyhedral *H* sheet is shown in square brackets, and that of the *HOH* layer is within braces; thus the composition of the interlayer is shown outside the braces.
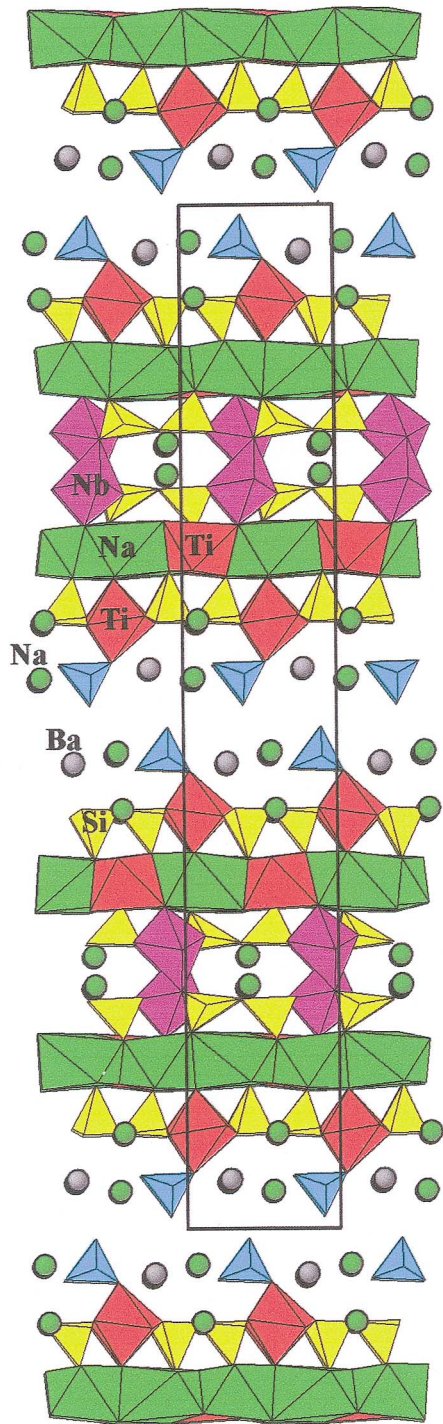
Pekov 2000) are reported in Table 3. As recently reviewed (Ferraris *et al.* 2001), all these minerals contain the bafertisite-like heterophyllosilicate layer. This type of layer can be derived from the tetrahedra – octahedra – tetrahedra (*TOT*) layer of the layer silicates by replacing [100] rows of disilicate groups $[Si_2O_7]^{6-}$ by rows of $[TiO_6]^{8-}$ octahedra. In some minerals, Ti has a coordination of 5 instead of 6; it can also be replaced by cations such as Nb, Zr and Na (Fig. 2, Table 3). The substituted *O* sheet becomes a *H* heteropolyhedral sheet, and the so-called bafertisite-like heterophyllosilicate *HOH* layer is thus obtained. It is characterized by ~5 × 7 Å two-dimensional periodicity in the (001) plane. In the *HOH* layer, two heteropolyhedral *H* sheets containing both tetrahedra and "octahedra" sandwich a more-or-less distorted sheet of octahedra in which various kinds of cations occur (Table 3). The various structures belonging to the bafertisite (or seidozerite) series consist of *HOH* layers that sandwich various kinds of anions and cations (Egorov-Tismenko 1998, Ferraris *et al.* 2001). The periodicity in the direction perpendicular to the *HOH* layer depends on the type of interlayer occupant. In particular, the structure of lomonosovite (Belov *et al.* 1978) consists of two *HOH* layers that sandwich $(PO_4)^{3-}$ tetrahedra and Na^+ (Fig. 2). In the structure of seidozerite (Simonov & Belov 1960), instead, two *HOH* layers link together because two adjacent Zr-bearing octahedra share an edge; the reduced interlayer space is occupied by Na^+ cations only (Fig. 2).

A comparison of the cell parameters shows that $c/2$ (23.97 Å) of bornemanite corresponds to the sum in thickness of one lomonosovite-like module (14.5 Å) and one seidozerite-like module (8.9 Å). Disregarding isomorphic substitutions (like Ba for Na and Nb for Ti), it turns out that half the sum of the crystal chemical-formulae of lomonosovite, $[Na_8\{(Na_2Ti_2)[Ti_2O_2$

TABLE 4. ATOM COORDINATES AND SITE OCCUPANCIES
IN BORNEMANITE

Atoms	x	y	z	Occupancy
Si1	0.440	0.124	0.280	1.0
Si2	0.362	0.573	0.287	1.0
Si3	0.726	0.361	0.391	1.0
Si4	0.675	0.783	0.399	1.0
P	0.360	0.891	0.459	1.0
Ti1	0.175	0.088	0.405	1.0
Ti2	0.835	0.608	0.336	1.0
Nb	0.890	0.878	0.270	0.7Nb + 0.3Ti
Na1	0.283	0.285	0.332	1.0
Na2	0.312	0.820	0.340	1.0
Na3	0.747	0.105	0.340	1.0
Na4	0.785	0.400	0.265	0.75Na + 0.25Mn
Na5	0.180	0.587	0.408	0.75Na + 0.25Mn
Na6	0.980	0.560	0.464	0.65Na + 0.35Ba
Ba	0.615	0.775	0.546	0.65Ba + 0.35Na
O1	0.410	0.352	0.280	1.0
O2	0.576	0.710	0.276	1.0
O3	0.735	0.119	0.283	1.0
O4	0.097	0.650	0.278	1.0
O5	0.258	-0.035	0.270	1.0
O6	0.492	0.583	0.317	1.0
O7	0.456	0.024	0.310	1.0
O8	0.900	0.860	0.314	1.0
O9	0.907	0.372	0.314	1.0
O10	0.726	0.563	0.407	1.0
O11	0.970	0.316	0.409	1.0
O12	0.942	0.863	0.404	1.0
O13	0.485	0.250	0.400	1.0
O14	0.430	0.892	0.409	1.0
O15	0.145	0.553	0.360	1.0
O16	0.105	0.051	0.365	1.0
O17	0.675	0.790	0.365	1.0
O18	0.648	0.408	0.359	1.0
O19	0.172	0.035	0.447	1.0
O20	0.415	0.688	0.449	1.0
O21	0.642	-0.109	0.460	1.0
O22	0.268	-0.109	0.489	1.0

$Si_4O_{14}](O,F)_2\}(PO_4)_2$, and seidozerite, $Na_2\{(Na,Mn,Ti)_4[(Na,Ti,Zr)_2O_2Si_4O_{14}]F_2\}$ (Table 3) corresponds well to the simplified crystal-chemical formula of
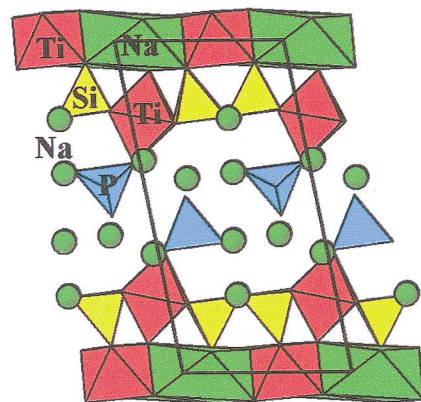
Fig. 2. Structural model of bornemanite compared with the structures of seidozerite and lomonosovite. The three structures are seen along [100], and the interlayer cations Na and Ba are shown as circles.
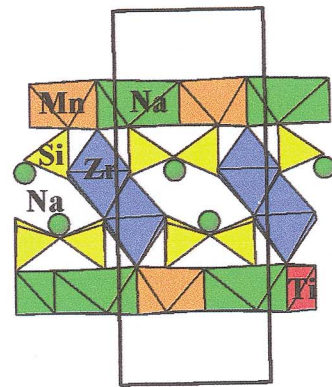
Seidozerite

Bornemanite

Lomonosovite

bornemanite $BaNa_3\{(Na,Ti)_4[(Ti,Nb)_2O_2Si_4O_{14}](F,OH)_2\}PO_4$.

Starting from the structures of lomonosovite and seidozerite, it was possible to build a structure model for bornemanite based on alternating seidozerite-like and lomonosovite-like modules (Fig. 2). In practice, the structure of bornemanite can be described as a [001] stack of *HOH* bafertisite-like heterophyllosilicate layers in which lomonosovite and seidozerite interlayer contents alternate. In Table 4, we report the atom coordinates, which have been refined to $R = 0.052$ by the DLS distance least-squares programme (Baerlocher *et al.* 1978). The DLS program optimizes the atom coordinates of a structure under constrained values of selected atomic distances.

A refinement of the structure by Rietveld method is impossible in practice because of the structural complexity of this species, with its 37 independent atoms. The structure model was tested by comparing calculated and observed intensities of the powder-diffraction pattern (Table 2) and, more qualitatively, of [100] and [001] SAED patterns (Fig. 1) using the Ca.R.Ine program by Boudias & Monceau (1998). An overall temperature-factor $B = 2$ Å^2 was used for the intensity calculations.

By trial and error, the best agreement between calculated and experimental powder-diffraction intensities was achieved under the following conditions for site occupancies (Table 4): (*i*) mixed occupancy of the interlayer sites by Na + Mn and Ba + Na; (*ii*) ordering of Ti and Nb within different *H* sheets, with mixed Nb + Ti occupancy in one site. The Ti/Nb order is related to two distinct roles of the octahedra in the *H* sheets; in fact, the Nb- and Ti-bearing octahedra occur in the seidozerite and lomonosovite modules, respectively. In bornemanite, two Nb-bearing octahedra of adjacent *H* sheets share a corner, whereas in seidozerite, the corresponding Zr-bearing octahedra share an edge. This different behavior can be attributed to the higher charge of Nb^{5+} compared to Zr^{4+}. Note that in bornemanite, as in other titanosilicates, Ti-bearing octahedra occur both in the *H* sheets (a corner is shared with PO$_4$ occurring in the interlayer) and in the octahedra of the *O* sheets. The main interatomic distances calculated with the coordinates of Table 4 are reported in Table 5.

The experimental distribution of intensities in the SAED patterns, obtained by incidence of the electron beam along [100] and [001], has been satisfactorily tested, even if only qualitatively, against the corresponding calculated patterns (Figs. 1b, e, f). As already mentioned, the calculation shows that owing to the small value of *c**, the SAED pattern along [001] corresponds to the intersection of the Laue sphere with *hk*0, *hk*1 and *hk*2 weighted reciprocal-lattice nodes. In the space group *I*11*b*, the expected diffraction-symmetry for the *hk*0 plane alone (Fig. 1e) is *p*2; instead, the presence of some local symmetry and the superposition of diffraction spots belonging to three reciprocal lattice planes produce an approximate *pmm* symmetry in the observed [001] SAED pattern (Figs. 1d, f). In the comparison between calculated and observed [001] SAED patterns, one must take into account that the calculated pattern (Fig. 1f) is a *projection* of the (*hk*0 + *hk*1 + *hk*2) slab of spherically weighted reciprocal-lattice nodes, whereas the observed pattern (Fig. 1d) is an *intersection* of the Laue sphere with [001] elongate nodes (spikes) bearing most of the diffracted intensity at their center. This effect is particularly evident for the 121 diffraction spot, which represents a clear disagreement between observed and calculated [001] SAED patterns.

CONCLUSIONS

The successful model of the structure of bornemanite represents a further example of the efficiency of the modular approach (Merlino 1997) in the investigation of minerals that do not offer single crystals suitable for X-ray crystallography (Ferraris *et al.* 1995, 1996, 1997, 1998, Ferraris 1997, Khomyakov *et al.* 1998). Chemical data, electron (SAED) and powder-diffraction patterns and a systematic comparison with known structures can provide the key for obtaining appropriate structure-models.

The structure of bornemanite is the first documented case containing modules of two different structures belonging to the same mero-plesiotype bafertisite series of layer titanosilicates, as defined by Ferraris *et al.* (2001). Thus, bornemanite is a polysome of a seidozerite–lomonosovite series. Ferraris *et al.* (2001) introduced the term mero-plesiotype series on the basis of

TABLE 5. SELECTED INTERATOMIC DISTANCES (Å) IN THE STRUCTURE MODEL OF BORNEMANITE

Si1 – O1	1.627	Si2 – O1	1.623	Si3 – O10	1.630	Si4 – O10	1.629
– O3	1.628	– O2	1.636	– O11	1.620	– O12	1.607
– O5	1.605	– O4	1.602	– O13	1.620	– O14	1.609
– O7	1.606	– O6	1.609	– O18	1.626	– O17	1.631
ave.	1.617	ave.	1.618	ave.	1.624	ave.	1.619

P – O19	1.546	Ti1 – O11	1.960	Ti2 – O6	2.106	Nb – O2	2.147
– O20	1.545	– O12	2.080	– O8	2.120	– O3	1.994
– O21	1.551	– O13	2.098	– O9	2.014	– O4	1.994
– O22	1.525	– O14	1.960	– O15	2.085	– O5	2.132
ave.	1.542	– O16	1.975	– O17	2.079	– O5	2.136
		– O19	2.049	– O18	2.094	– O8	2.114
		ave.	2.020	ave.	2.083	ave.	2.086

Na1 – O1	2.636	Na2 – O6	2.225	Na3 – O3	2.732	Na4 – O1	2.219
– O6	2.545	– O7	2.207	– O7	2.229	– O1	2.287
– O7	2.318	– O8	2.594	– O8	2.285	– O2	2.516
– O9	2.309	– O15	2.340	– O9	2.457	– O3	2.203
– O15	2.437	– O16	2.309	– O16	2.327	– O4	2.583
– O16	2.516	– O17	2.333	– O17	2.583	– O9	2.450
– O18	2.563	ave.	2.335	– O18	2.391	ave.	2.376
ave.	2.475			ave.	2.429		

Na5 – O10	2.507	Na6 – O10	3.069	Ba – O10	3.119
– O11	2.277	– O11	3.159	– O11	2.930
– O12	2.338	– O20	2.681	– O13	2.693
– O14	2.603	– O21	2.966	– O19	3.033
– O15	2.323	– O22	3.116	– O20	3.120
– O20	2.470	– O22a	2.988	– O21	2.749
ave.	2.420	ave.	2.997	ave.	2.941

Makovicky's (1997) definition for a merotype series (at least a building module is common to all members of the series, but each member also can show peculiar modules) and a plesiotype series (the building modules of the series may differ for some parts in specific members). In fact, the bafertisite series contains aspects of both merotype and plesiotype series. Difficulties in preparing TEM mounts with the *HOH* layer parallel to the incident beam did not allow us so far to check for the occurrence of polysomes as stacking faults of the matrix structures.

The presence of the same *HOH* layer in the structures of bornemanite and lomonosovite explains well the oriented growth of the first species on the second one, mentioned earlier. Taking into account the complete substitution of lomonosovite by bornemanite reported by Pekov (2000), the lamellar bornemanite occurring in our sample can be interpreted as a secondary phase that formed from lomonosovite by a topotactic reaction. This reaction is consequent to a destabilization that leads to cation leaching and exchange in the interlayer of the primary lomonosovite. Several cases of reactions that generate secondary phases by preserving either the full *HOH* layer [lomonosovite + $H_2O \rightarrow$ murmanite + (Na + P); vuonnemite + $H_2O \rightarrow$ epistolite + (Na +P)] or the *H* sheet only [parakeldyshite → keldyshite] are reported by Khomyakov (1995). They have been interpreted by Ferraris (1997) as solid-state phenomena connected with the modular structures.

Note that in the case of bornemanite, the thickness $t = d(001)/n$, as defined in the footnote to Table 3, is no longer indicative of the complexity of a single interlayer, but depends on the presence of two different types of content in the interlayers. The modeling of the bornemanite structure broadens the versatile role of the *HOH* bafertisite-like layer. In fact, now this layer is known in the heterophyllosilicates, where it occurs together with astrophyllite-like and nafertisite-like *HOH* layers (Christiansen *et al*. 1999, Ferraris *et al*. 1996), in the seidozerite–lomonosovite polysomatic series (this work), and in the complex mero-plesiotype bafertisite series (Ferraris *et al*. 2001) mentioned above.

In addition to being a contribution to the mineralogy of hyperalkaline rocks and the crystal chemistry of inorganic compounds, knowledge of the large variety of structures offered by the alkaline titanosilicates also can benefit applied science, as shown by an increasing interest in technological applications of derived structures. In fact, as recently reviewed by Rocha & Anderson (2000), several synthetic and natural titanosilicates show properties typical of the so-called microporous materials (molecular sieves) and can be used, for example, in catalytic processes.

ACKNOWLEDGEMENTS

The authors are grateful to referees U. Kolitsch and L. Karanović, Associate Editor O. Johnsen and R.F.

REFERENCES

BAERLOCHER, C., HEPP, A. & MEIER, W.M. (1978): *Manual DLS–76. A Program for the Simulation of Crystal Structures by Geometric Refinement*. ETH, Zürich, Switzerland.

BELOV, N.V., GAVRILOVA, G.S., SOLOV'EVA, L.P. & KHALILOV, A.D. (1978): The refined structure of lomonosovite. *Sov. Phys. Dokl.* **22**, 422-424.

BOUDIAS, C. & MONCEAU, D. (1998): *Ca.R.Ine Crystallography 3-1 for Microsoft Windows – User Manual*. Ca.R.Ine Crystallography, Senlis, France.

CHRISTIANSEN, C.C., MAKOVICKY, E. & JOHNSEN, O.N. (1999): Homology and typism in heterophyllosilicates: an alternative approach. *Neues Jahrb. Mineral., Abh.* **175**, 153-189.

EGOROV-TISMENKO, YU.K. (1998): On the seidozerite–nacaphite polysomatic series of minerals: titanosilicate analogues of mica. *Crystallogr. Rep.* **43**, 271-277.

ERCIT, T.S., COOPER, M.A. & HAWTHORNE, F.C. (1998): The crystal structure of vuonnemite, $Na_{11}Ti^{4+}Nb_2(Si_2O_7)(PO_4)_2 O_3(F,OH)$, a phosphate-bearing sorosilicate of the lomonosovite group. *Can. Mineral.* **36**, 1311-1320.

FERRARIS, G. (1997): Polysomatism as a tool for correlating properties and structure. *In* Modular Aspects of Minerals (S. Merlino, ed.). *Eur. Mineral. Union, Notes in Mineralogy* **1**, 275-295.

————, IVALDI, G., KHOMYAKOV, A.P., SOBOLEVA, S.V., BELLUSO, E. & PAVESE, A. (1996): Nafertisite, a layer titanosilicate member of a polysomatic series including mica. *Eur. J. Mineral.* **8**, 241-249.

————, ————, PUSHCHAROVSKY, D.YU., ZUBKOVA, N.V. & PEKOV, I.V. (2001): The crystal structure of delindeite, $Ba_2\{(Na,K,\square)_3(Ti,Fe)[Ti_2(O,OH)_4Si_4O_{14}] (H_2O,OH,O)_2\}$, a member of the mero-plesiotype bafertisite series. *Can. Mineral.* **39**, 1307-1316.

————, KHOMYAKOV, A.P., BELLUSO, E. & SOBOLEVA, S.V. (1997): Polysomatic relationship in some titanosilicates occurring in the hyperagpaitic alkaline rocks of the Kola Peninsula, Russia. *Proc. 30th Int. Geol. Congress* **16**, 17-27.

_____, _____, _____ & _____ (1998): Kalifersite, a new alkaline silicate from Kola Peninsula (Russia) based on a palygorskite–sepiolite polysomatic series. *Eur. J. Mineral.* **10**, 865-874.

_____, PAVESE, A. & SOBOLEVA, S.V. (1995): Tungusite: new data, relationship with gyrolite and structural model. *Mineral. Mag.* **59**, 535-543.

KHOMYAKOV, A.P. (1995): *Mineralogy of Hyperagpaitic Alkaline Rocks*. Clarendon Press, Oxford, U.K.

_____, FERRARIS, G., BELLUSO, E., BRITVIN, S.N., NECHELYUSTOV, G.N. & SOBOLEVA, S.V. (1998): Seidite-(Ce), $Na_4SrCeTiSi_8O_{22}F•5H_2O$, a new mineral with zeolitic properties. *Zap. Vser. Mineral. Obshchest.* **127**(4), 94-100 (in Russ.).

_____, NECHELYUSTOV, G.N., SOKOLOVA, E.V. & DOROKHOVA, G.I. (1992): Quadruphite $Na_{14}CaMgTi_4$ $[Si_2O_7]_2[PO_4]_2O_4F_2$ and polyphite $Na_{17}Ca_3Mg(Ti,Mn)_4$ $[Si_2O_7]_2[PO_4]_6O_2F_6$, two new minerals of the lomonosovite group. *Zap. Vser. Mineral. Obshchest.* **121**(3), 105-112 (in Russ.).

MAKOVICKY, E. (1997): Modularity – different types and approaches. *In* Modular Aspects of Minerals (S. Merlino, ed.). *Eur. Mineral. Union, Notes in Mineralogy* **1**, 315-344.

MEN'SHIKOV, YU.P., BUSSEN, I.V., GOIKO, E.A., ZABAVNIKOVA, N.I., MER'KOV, A.N. & KHOMYAKOV, A.P. (1975): Bornemanite – a new silicophosphate of sodium, titanium, niobium and barium. *Zap. Vser. Mineral. Obshchest.* **104**, 322-326 (in Russ.).

MERLINO, S., ed. (1997): *Modular Aspects of Minerals.* The European Mineralogical Union, Notes in Mineralogy **1**.

PEKOV, I.V. (2000): *Lovozero Massif.* Ocean Pictures Ltd., Moscow, Russia.

PENG, ZHIZHONG, ZHANG, JIANHONG & SHU, JINFU (1984): The crystal structure of barytolamprophyllite and orthorhombic lamprophyllite. *Kexue Tongbao* **29**, 237-241.

RASTSVETAEVA, R.K. & ANDRIANOV, V.I. (1986): New data on the crystal structure of murmanite. *Sov. Phys. Crystallogr.* **31**, 44-48.

_____, SOKOLOVA, M.N. & GUSEV, A.I. (1990): Refined crystal structure of lamprophyllite. *Mineral. Zh.* **12**(5), 25-28.

ROCHA, J. & ANDERSON, M.W. (2000): Microporous titanosilicates and other novel mixed octahedral–tetrahedral framework oxides. *Eur. J. Inorg. Chem.*, 801-818.

SIMONOV, V.I. & BELOV, N.V. (1960): The determination of the structure of seidozerite. *Sov. Phys. Crystallogr.* **4**, 146-157.

SOKOLOVA, E.V., EGOROV-TISMENKO, YU.K. & KHOMYAKOV, A.P. (1988): The crystal structure of sobolevite. *Sov. Phys. Dokl.* **33**, 711-714.